Research Square

Preprints are preliminary reports that have not undergone peer review.
They should not be considered conclusive, used to inform clinical practice,
or referenced by the media as validated information.

Superhydrophobic encapsulation of flexible Bi2Te3/CNT coated thermoelectric fabric via layer-by-layer assembly

Ding Ding
Xi'an Polytechnic University
Qian Wu (Qian_Ng@outlook.com)
Xi'an Polytechnic University
Jinmei Wang
Key Laboratory of Functional Textile Material and Product (Xi'an Polytechnic University)
Yixun Chen
Xi'an Polytechnic University
Qian Li
Xi'an Polytechnic University
Lin Hou
Shaanxi Textile Research Institute Co., Ltd
Lei Zhao
Shaanxi Textile Research Institute Co., Ltd
Yan-yan Xu
Shaanxi Textile Research Institute Co., Ltd

Research Article

Keywords: thermoelectric, fabric, flexible electronics, superhydrophobic, CNT, Bi2Te3

Posted Date: September 23rd, 2022

DOI: https://doi.org/10.21203/rs.3.rs-2074561/v1

License: This work is licensed under a Creative Commons Attribution 4.0 International License.
Read Full License

Abstract

Fabric based flexible thermoelectric materials capable of converting body heat to electricity are promising in self-powered wearable electronic applications. To improve the thermoelectric performance and the wearability of fabric based thermoelectric materials, a superhydrophobic encapsulated Bi_2Te_3/CNT thermoelectric fabric was introduced. Through layer-by-layer assembly process, Bi_2Te_3 and CNT were coated onto the surface of cotton fabric substrate, respectively. The prepared thermoelectric fabric has great flexibility and a power factor of 0.15μW·m^{-1}·K^{-2}. A thermoelectric generator consists of five Bi_2Te_3/CNT fabric legs could generate an output voltage of 1.8mV under a temperature difference of 30°C and could be easily attached to the end of sleeves or socks. A double layer superhydrophobic encapsulation composed of silicone, PDMS and PMMA was coated onto the surface of Bi_2Te_3/CNT fabric to isolated it from the ambient environment. The encapsulation layer, with a water contact angle of 158.6° and a sliding angle of 6.5°, exhibits great self-cleaning property and flexibility. This concept of superhydrophobic thermoelectric fabric paves new way to improve the durability and wearability of thermoelectric generators.

Introduction

Flexible thermoelectric materials and devices are regarded as promising power supplies for wearable electronics since they can convert human body heat into electricity(Ding et al., 2021; H. Li et al., 2021; M. Li et al., 2020; Lund et al., 2020; Nuthongkum et al., 2017). Fabrics with great flexibility, breathability, and wearing comfort are more suitable for wearable applications than widely studied thermoelectric films(Gao et al., 2021; Ma et al., 2021; Tan et al., 2018; X. Wu & Wen, 2021). By converting human body heat, a thermoelectric fabric is possible to provide sustained power for a wearable electronic system(Allison & Andrew, 2019; Kim et al., 2022; G. Liu & Qiao, 2015; Park et al., 2021). However, the low efficiency and lack of proper encapsulation limited the practicability of fabric based flexible thermoelectric materials for wearable applications. Generally, the performance of a thermoelectric fabric is usually evaluated by the thermoelectric figure of merit $ZT = \frac{\sigma S^2}{K} T$, where σ represents the electrical conductivity, S represents the Seebeck coefficient, T represents the absolute temperature difference, and K is the thermal conductivity(Poudel et al., 2008). In some cases, the power factor (σS^2) can also be used to evaluate the performance of a thermoelectric fabrics when the effect of the thermal conductivity of the material is of secondary importance(Q. Wu & Hu, 2016).

Currently, most thermoelectric fabrics were produced by incorporating organic thermoelectric materials with flexible fabric substrates(Culebras et al., 2020; Du et al., 2017; Maria et al., 2021; Wei et al., 2022; Zhang et al., 2020). For example, Du et al. directly coated commercial available poly(3,4 ethylenedioxythiophene):poly(styrenesulfonate) (PEDOT:PSS) on polyester and cotton fabrics respectively as thermoelectric fabrics via a solution coating process, and obtained a maximum power factor of 0.5μW·m^{-1}·K^{-2} (Du et al., 2020). Paleo et al adopted a dip coating method to coat a cotton

fabric with vapor grown carbon nanofiber based inks. The prepared thermoelectric fabric exhibited a power factor of 1.65×10^{-3} $\mu W \cdot m^{-1} \cdot K^{-2}$(Paleo et al., 2020). Although organic thermoelectric materials are flexible and have relatively low thermal conductivity, their ZT values are lower than those of inorganic thermoelectric materials. Bi_2Te_3 is a typical inorganic thermoelectric material widely used for room temperature conversion(Y. Liu et al., 2016). By introducing Bi_2Te_3 onto a flexible substrate, the thermoelectric performance of the substrate is expected to be enhanced. Liu et al. fabricated a thin-film flexible thermoelectric device by depositing p-type and n-type Bi_2Te_3 onto the surface of polyimide/copper substrates via electronic deposition technology. The device exhibited an output voltage of 97.5 mV and the maximum power of 60 μW at a temperature difference of 80 K.(C. Liu et al., 2021)

However, most of these inorganic thermoelectric coatings are conducted on flexible film substrates rather than fabric substrates(Chen et al., 2021; Ferhat et al., 2019; Jin et al., n.d.; Varghese et al., 2019; Zhao et al., 2020). Considering the roughness and porous structures of fabric surfaces, only coating them with these inorganic thermoelectric particles cannot form a continuous conductive network on the fabric substrate, thus resulting in a lower thermoelectric performance than film thermoelectric materials. Additionally, the interfacial interactions between inorganic thermoelectric particles and fabric substrates are usually weak, which made the coatings easily peel off under the action of external forces. In real wearable situations, thermoelectric fabrics will be exposed to the ambient environment. Without good encapsulation, the coatings are vulnerable to the wet and corrosive conditions, which is detrimental to their thermoelectric performance. These problems are widely existed in many flexible thermoelectric materials fabricated by coating technique.

In this work, we report a superhydrophobic encapsulated multi-walled carbon nanotube (MWCNT)/ Bi_2Te_3 thermoelectric fabric prepared by layer-by-layer (LbL) assembly technique. Cotton fabric was used as flexible substrate. MWCNTs and Bi_2Te_3 were coated respectively on the surface of the cotton substrate to prepare thermoelectric fabric. A double layer superhydrophobic encapsulation composed of silicone, PDMS and PMMA was constructed on the MWCNTs/ Bi_2Te_3 coated thermoelectric fabric. In this multi-layer composite structure, MWCNTs were used to create conductive networks on the cotton fabric substrate, the addition of Bi_2Te_3 particles contributed to the enhancement of thermoelectric performance, and the superhydrophobic encapsulation was acted as protective layer to improve the durability and reliability of the thermoelectric fabric in harsh operational environments. The concept of constructing this multi-layer hierarchical structure on cotton fabric substrate is a facile and effective way to prepare flexible superhydrophobic thermoelectric fabrics.

Experimental

Materials

Commercially available cotton fabric with area density of 256 g/m^2 was purchased from Fuzhou Hongda Textile Co. LTD. MWCNT was purchased from Sigma-Aldrich (110-170nm in diameter, length 5-9μm,

Carbon basis>90%). Bi_2Te_3 (mass fraction:99.99%) was purchased from Shanghai Aladdin Biochemical Technology Co. LTD. Sylgard 184 Silicone Elastomer Kit with components of PDMS base and curing agent, was purchased from Dow Corning Co., Ltd. Polymethylmethacrylate (PMMA) was purchased from Shunjie Plastic Technology Co. LTD. Silica gel was purchased from Foshan xin boqiao Electronics Co., LTD. Sodium hydroxide (NaOH), Waterborne Polyurethane (WPU), sodium dodecyl benzene sulfonate (SDBS) and Tetrahydrofuran (THF) were purchased from Tianjin Damao Chemical Reagent Factory. All the chemicals were used as received without further purification.

Fabrication of the Bi_2Te_3/MWCNTs thermoelectric fabrics

Firstly, MWCNTs-coated cotton fabrics (CCF) were prepared by a drop-coating process. Prior to drop-coating, the cotton fabrics (3cm×3cm) was immersed in a NaOH solution to remove contaminants and improve adhesion between the fabric substrate and the coating layer. Then, WPU (mass fraction:10%) was added to the surface of fabric substrate to improve the adhesion between the MWCNTs and cotton fabrics. MWCNTs were dispersed in water by sonication for 40 min with the aid of SDBS. The weight ratio of SDBS and MWCNTs was 1:1. Subsequently, the MWCNTs dispersion was dropped onto the surface of cotton fabric substrate, followed by drying at 80℃ for 30min to obtain CCF. The CCF with different MWCNTs areal density was prepared by controlling the dosage of MWCNTs dispersion onto the fixed area of cotton fabric. Secondly, Bi_2Te_3/MWCNTs-coated cotton fabrics (Bi_2Te_3/CCF) were prepared by a physical vapor deposition (PVD) process. A thermal evaporation coating device (ZD-500B) was employed to evaporate the Bi_2Te_3 particles onto the surface of CCF. The vacuum chamber was evacuated down to a base pressure of 2.0×10^{-3}Pa before the deposition. The evaporation voltage was adjusted to 30V, and the total deposition time was 120s. The influence of deposition times on the properties of the Bi_2Te_3/CCF was systematically investigated. For convenience, the Bi_2Te_3/CCF with different deposition times of Bi_2Te_3 are marked as Bi_2Te_3/CCF-X respectively, and the value of X represents the deposition times.

Superhydrophobic encapsulation of the Bi_2Te_3/MWCNT thermoelectric fabrics

The superhydrophobic encapsulation of Bi_2Te_3/CCF was achieved by constructing a composite coating on the surface of the Bi_2Te_3/CCF sample. Firstly, the silica gel solution was applied to the surface of the Bi_2Te_3/CCF sample, and the silica gel coated fabric could be obtained after drying. Secondly, PDMS and PMMA, with a weight ratio of 1:1, were dispersed in 25 ml THF solvent, which was stirred for 2 h to accelerate dissolution. Subsequently, it was sprayed on the surface of the silica gel coated Bi_2Te_3/CCF with a spray gun under a pressure of 0.2 MPa. Then, a superhydrophobic surface can be achieved immediately without any additional processing.

Characterization and measurement

The micro morphologies and compositions of the fabric were investigated by using field-emission scanning electron microscopy (FE-SEM), which was equipped with energy-dispersive X-ray spectroscopy (EDS). The electrical conductivity of the prepared fabric samples (3×3 cm^2) was measured by a four-point

probe apparatus (ST2253, Suzhou Jingge Electron, China). A homemade device was employed to characterize the generated thermal voltage under different temperature gradients. The thermal voltage was measured by a Keithley DMM6500 digital multimeter. Two K-type thermocouples were used to measure the temperatures of the hot side and the cold side respectively. The Seebeck coefficient can be calculated from the slope of the voltage versus temperature difference (DT) curves. The water resistance properties of the sample were investigated by water contact angle measurement (OCA50, Dataphysics, Germany).

Result And Discussion

A lay-by-layer assembly process was used to prepare a superhydrophobic encapsulated MWCNTs/Bi_2Te_3 thermoelectric fabric. As illustrated in Fig. 1(a), MWCNTs dispersions were uniformly drop-coated on the cotton fabric substrate to construct a primary conductive network on the surface of the fabric. Then, Bi_2Te_3 particles were deposited upon the MWCNTs conductive networks via a PVD process. To minimize the decreasing of electrical conductivity during deformation, MWCNTs with high aspect ratio are appropriate for constructing effective conductive networks on flexible substrate. The inorganic Bi_2Te_3 particles decorated along the surface of MWCNTs can enhance the Seebeck coefficient of the coated cotton fabric. Thus, the conversion performance of the designed flexible thermoelectric fabric is expected to be improved. A double layer encapsulation was applied to fabricate the superhydrophobic thermoelectric fabric. A silicone with Shore 20A was coated onto the surface of Bi_2Te_3/CCF sample to obtain the first protection layer. Then, the second superhydrophobic layer was fabricated by spraying the dispersion of PDMS and PMMA in THF on the silicone layer. The low surface energy and the microscale roughness of PDMS/PMMA coating synergistically contributed to the superhydrophobic and self-cleaning effect of the thermoelectric fabric. It should be noticed that direct coating the PDMS/PMMA on the Bi_2Te_3 surface cannot obtain the superhydrophobic effect, and furthermore, it also reduces the performance of thermoelectric layer. The PDMS (Sylgard 184 Silicone) used for superhydrophobic coating has a hardness of 43A, which would lead to a severe cracking phenomenon on Bi_2Te_3 layer and the difficult spreading out of PDMS dispersions on the Bi_2Te_3 surface. By introducing the Shore 20A silicone as a middle protection layer, the cracking of Bi_2Te_3 layer was reduced significantly, and the PDMS superhydrophobic coating can be successfully formed.

The photograph of the prepared CCF, Bi_2Te_3/CCF, and P-Bi_2Te_3/CCF samples are shown in Fig.1 (b)-(d) respectively. The CCF conductive fabric is black and can be folded at any angle, which was attributed to the flexibility of cotton fabric substrate. After the thermal evaporation of Bi_2Te_3, the color of the Bi_2Te_3/CCF have turned to silver grey, suggesting that the Bi_2Te_3 powders have been successfully decorated on the surface of CCF, and the Bi_2Te_3/CCF remained flexible. Since the double layer superhydrophobic encapsulation is transparent and flexible, the P- Bi_2Te_3/CCF strip exhibits the same silver grey color and can be easily twisted without being damaged.

The SEM images of original cotton fabrics (Fig. S1(a, b)), CCF (Fig. 2(a-c)), Bi_2Te_3/CCF (Fig. (d-f)) and P-Bi_2Te_3/CCF (Fig.(g-i)) were observed, respectively. Fig. 2 (a) and (b) exhibit the surface structure of CCF, and the cross-section structure is shown in Fig.2 (c). It can be observed that MWCNTs with high aspect ratios were randomly connected and uniformly coated on the surface of cotton fabric substrate. Thus, the primary conductive network was formed. The surface and cross-section structures of Bi_2Te_3 coating layer are shown in Fig. 2 (d-f), indicating that Bi_2Te_3 particles were successively deposited on the surface of MWCNTs. The surface and cross-section structures of the PDMS/PMMA superhydrophobic coating are shown in Fig.2 (g-i). The microscale rough surface was achieved by distributing polymer particles in the coating layer, which contributed to the superhydrophobic performance of the encapsulation layer.

X-ray energy dispersive spectrum was used to express the surface elements of the prepared CCF, Bi_2Te_3/CCF and P- Bi_2Te_3/CCF samples, respectively. As shown in Fig. 2(j), compared with the original cotton fabric (Fig S2), the surface element species of the CCF sample remained the same, but the content of C element increased significantly, from 55.41wt% to 64.48wt%, which was attributed to the adhesion of MWCNTs. In contrast, as shown in Figure 2(k), the Bi and Te peaks appeared on the surface of Bi_2Te_3/CCF, and the contents of C, O, Bi and Te elements were 25.61wt%, 7.29wt%, 11.23wt% and 55.86wt% respectively, which indicates the successful coating of Bi_2Te_3 on the CCF surface. Figure 2 (l) shows the surface elements of P- Bi_2Te_3/CCF. The peaks of Bi and Te disappeared, replaced by the appearance of Si peaks, which indicates the Bi_2Te_3/CCF was well encapsulated by the superhydrophobic coating of silicone and PDMS. Furthermore, the elemental distribution of these samples showed that MWCNTs, Bi_2Te_3 and PDMS/PMMA were uniformly covered the fabric substrate.

To further investigate the thermoelectric properties of the prepared Bi_2Te_3/CCF, the electrical conductivity, Seebeck coefficient, and power factor at room temperature were observed and calculated respectively. The thermoelectric performances of Bi_2Te_3/CCF with different deposition times of Bi_2Te_3 powder are shown in Fig.3 (a) and (b). It can be observed that both electrical conductivity and Seebeck coefficient of the Bi_2Te_3/CCF samples were enhanced with the increased times of Bi_2Te_3 deposition. Obviously, Bi_2Te_3 as an inorganic semiconductor has excellent thermoelectric performance at room temperature. The more times of deposition would increase the coating contents of Bi_2Te_3 on CCF surface, which resulted in the enhancement of electrical conductivity and Seebeck coefficient. However, the electrical conductivity of the Bi_2Te_3/CCF sample was decreased at fifth times of deposition. This result implies that further increasing the number of Bi_2Te_3 deposition times cannot continuously increase the thermoelectric performance. Since the Bi_2Te_3 is a rigid semiconductor lack of flexibility, a thicker Bi_2Te_3 coating layer is prone to crack, which would lead to the breaking of electrical connections. The SEM images of Bi_2Te_3/CCF under different times of Bi_2Te_3 deposition (Fig. S3) proved that Bi_2Te_3 coating layers were gradually thickening with increased number of deposition times. Although the Seebeck coefficient of Bi_2Te_3/CCF-5 sample was still increased, the overall power factor of the sample was decreased due to the reduced electrical conductivity. Therefore, the optimal power factor of 0.15 $\mu W \cdot m^{-1} \cdot K^{-2}$ was achieved by Bi_2Te_3/CCF-4 sample.

The heat transfer performance of the sample Bi_2Te_3/CCF-4 was visualized using a temperature-sensitive paint which was red at room temperature and turned yellow when the temperature was above 40 °C. As shown in Fig. 3(c), the two ends of the sample with a length of 4.5cm and a width of 2cm were placed on the surface of two copper blocks, and then the left copper block was heated to 45 °C, while the temperature of the right copper block was kept at room temperature. The sample was placed in physical contact with the copper block so that the heat of the copper block can transfer laterally along the sample to change the color of the temperature-sensitive paint. After heating the left side of the sample for 2 hours, the temperature-sensitive paint on the right side of the sample remained red (Fig.3(c)). As shown in movie S1, the hot end of thermochromic paint was slowly extended about 0.3cm toward the cold end during the 2 hours heating. It demonstrated that the prepared Bi_2Te_3/CCF-4 sample has limited in-plane heat transfer, which is conducive to the heat-to-electricity conversion process.

In wearable application, flexible thermoelectric devices without proper encapsulation are easily damaged by external environment. Oxidation and pollution will reduce the performance of the devices. To overcome these obstacles for real application, superhydrophobic encapsulation of flexible fabric based thermoelectric materials was introduced. The evolution of surface hydrophilicity for the thermoelectric fabric Bi_2Te_3/CCF, Silicone coated fabric SC- Bi_2Te_3/CCF and superhydrophobic fabric P-Bi_2Te_3/CCF was investigated. As shown in Fig. 4 (a), the water contact angle (CA) was converted from 0.3° to 114.2° after encapsulation of the thermoelectric fabric Bi_2Te_3/CCF with silicone, resulting in a hydrophobic effect. The silica gel coating forms a translucent film on the surface of the thermoelectric fabric Bi_2Te_3/CCF (Fig. S4). It is worth noting that the hardness of silicone used here is 20A. The Bi_2Te_3 coating layer encapsulated with higher hardness silicone would be cracked severely. To further achieve the superhydrophobic effect, the dispersion of PDMS and PMMA in THF was sprayed onto the surface of 20A silicone encapsulated fabric. Hence, the surface roughness of the encapsulation layer could be increased, resulted in a superhydrophobic stain repellent coating. Generally, a surface with water contact angle higher than 150° is considered to have superhydrophobic property. As shown in Fig. 4 (a), the water contact angle of P-Bi_2Te_3/CCF was increased to 158.6°, indicating that the prepared encapsulation layer has superhydrophobic performance. P-Bi_2Te_3/CCF also showed low hysteresis with a small sliding angle (SA) of 6.5°, indicating the low surface adhesion (Fig 4 (b)). When other liquid droplets such as water, milk, and coffee were dropped on the surface of the P- Bi_2Te_3/CCF, the droplets steadily stood on the surface rather than permeating the thermoelectric fabric (Fig. S5(a)). Therefore, the stains in daily life could be easily removed from the surface of the encapsulated thermoelectric fabric with rinse (Fig. S5(b)). Besides, the encapsulated sample exhibits superior mechanical flexibility. As shown in Fig. 4(c) and (d), the P- Bi_2Te_3/CCF-4 sample can be easily bended and twisted. With the self-cleaning property and great flexibility, the thermoelectric fabric can be used in various daily wearable applications.

Meanwhile, the impact of the superhydrophobic encapsulation, mechanical deformation, and chemical solvents on the thermoelectric performance of P-Bi_2Te_3/CCF-4 sample were evaluated. As shown in Fig. 4(e), compared with the original Bi_2Te_3/CCF-4 sample without encapsulation, the Seebeck coefficient of

the P- Bi_2Te_3/CCF sample was only slightly decreased from 20.26μv/k to 19.82μv/k, which indicated that the double layer superhydrophobic coating had little negative effect on the original thermoelectric performance. To investigate the mechanical durability, the P-Bi_2Te_3/CCF-4 sample was bended with a distorted radius of 2.0mm and twisted with a torsion angle of 360° respectively. After 100 bending-release cycles and 100 torsional-release cycles, P- Bi_2Te_3/CCF maintained excellent Seebeck coefficients of 18.62μv/k and 18.38μv/k, respectively, which indicated that the P- Bi_2Te_3/CCF had excellent mechanical flexibility and durability. To overcome the adverse impact of harsh environment, the thermoelectric fabric needs to have certain chemical resistance. To investigate the influence of chemicals on the Seebeck coefficient, P- Bi_2Te_3/CCF-4 sample was immersed in acid (pH = 2.0), alkali (pH = 12.0), ethanol, formaldehyde, and propanol respectively for 10 h. As shown in Fig. 4(f), the Seebeck coefficient of the P-Bi_2Te_3/CCF-4 sample after immersed with the above chemicals was still higher than 18.83μv/k, indicating that these chemicals have no obvious impact on thermoelectric performance of the sample. Hence, the prepared superhydrophobic thermoelectric fabric exhibits great mechanical flexibility and chemical resistance that could ensure long-term durability in daily life wearable situations, even in harsh environments.

To demonstrate the potential of the P-Bi_2Te_3/CCF thermoelectric fabric for wearable application, a fabric TEG with 5 legs was fabricated. As shown in Fig. 5(a), five rectangular P- Bi_2Te_3/CCF strips with the size of 3×0.6cm (L×W) were used as P-type legs and connected in series with copper wire. Copper foils were adhered to the two ends of P- Bi_2Te_3/CCF strips to improve the electrical connection stability between the copper wires and P-type legs. To evaluate the output performance of TEG, one side of the TEG was heated, and the other side was exposed to the ambient atmosphere. As the temperature difference increased from 5℃ to 30℃, the corresponding output voltage and output power were measured. As shown in Fig. 5(b), an output voltage of 1.8 mV and output power of 1.6 nW were obtained at a temperature difference of 30℃. Besides, the prepared wearable TEG can be folded and attached to the end of sleeves or socks, as shown in Fig. 5 (c). In this design, one side of the TEG can be in contact with the skin or placed at the inner layers of clothes, while the other side can be exposed to the environment. Generally, wearable devices are easily affected by the surrounding environment in practical applications. For example, when the TEG is placed on the wrist or ankle, it will be easily contaminated by sweat or rain. In this case, the superhydrophobic encapsulation can improve the durability and practical application value of thermoelectric fabrics.

Conclusion

In this study, Bi_2Te_3 and MWCNTs were coated on a cotton fabric substrate via layer-by-layer assembly process to fabricate thermoelectric fabric. The prepared P- Bi_2Te_3/CCF sample has an optimal power factor of 0.15 $\mu W \cdot m^{-1} \cdot K^{-2}$ and could maintain its high Seebeck coefficient after 100 bending release cycles and 100 twisting release cycles, respectively. To improve the wearability, a double layer superhydrophobic encapsulation were added to the thermoelectric fabric. A high CA of 158.6° and a low SA of 6.5° can be achieved by the encapsulation layer, indicating its excellent superhydrophobic property.

Besides, the P- Bi_2Te_3/CCF exhibits great resistance to acid/alkali solutions as well as organic solvents. Finally, a flexible TEG composed of five thermoelectric legs was fabricated to demonstrate the power generation performance and practical wearability. An output voltage of 1.8 mv and output power of 1.6nw were obtained. With great flexibility, the TEG could be easily worn on wrist or ankle. The self-cleaning effect of superhydrophobic encapsulation improves the durability and wearability of this fabric TEG. It is believed that this work provides novel design ideas for the development of high performance superhydrophobic thermoelectric fabric.

Declarations

Ethics approval and consent to participate

Compliance with ethical standards.

Consent for publication

All authors approved the final manuscript and the submission to this journal.

Availability of data and materials

The datasets generated or analyzed during this study are available from the corresponding author on reasonable request.

Competing interests

There are no conflicts to declare.

Funding

This work was supported by the Scientific Research Program Funded by Education Department of Shaanxi Provincial Government (Program No. 22JK0395); Science and Technology Guiding Project of China National Textile Industry Council (Grant No. 2020043); Natural Science Basic Research Plan in Shaanxi Province of China (Program No. 2022GY-283); Engineering Technology Research Center of Textile for Safety Protection in Shaanxi Province (Grant No. 2021CXYHZ-006); and Xi'an Polytechnic University Start-up Research fund (Grant No. 107020349).

Authors' contributions

All the authors participated, discussed the results, and reviewed the manuscript.

Acknowledgements

Not applicable

References

1. Allison, L. K., & Andrew, T. L. (2019). A Wearable All-Fabric Thermoelectric Generator. Advanced Materials Technologies, *4*(5), 1–7. https://doi.org/10.1002/admt.201800615
2. Chen, X., Feng, L., Yu, P., Liu, C., Lan, J., Lin, Y., & Yang, X. (2021). *Flexible Thermoelectric Films Based on Bi 2 Te 3 Nanosheets and Carbon Nanotube Network with High n − Type Performance*. https://doi.org/10.1021/acsami.0c21396
3. Culebras, M., Sanchis, M. J., Serrano-claumarchirant, J. F., & Brotons-alca, I. (2020). *Electrochemical Synthesis of an Organic Thermoelectric Power Generatoŕ*. https://doi.org/10.1021/acsami.0c12076
4. Ding, T., Zhou, Y., Wang, X. Q., Zhang, C., Li, T., Cheng, Y., Lu, W., He, J., & Ho, G. W. (2021). All-Soft and Stretchable Thermogalvanic Gel Fabric for Antideformity Body Heat Harvesting Wearable. Advanced Energy Materials, *11*(44), 1–9. https://doi.org/10.1002/aenm.202102219
5. Du, Y., Tian, T., Meng, Q., Dou, Y., Xu, J., & Shen, S. Z. (2020). Thermoelectric properties of flexible composite fabrics prepared by a gas polymerization combining solution coating process. *Synthetic Metals*, *260*(November 2019), 116254. https://doi.org/10.1016/j.synthmet.2019.116254
6. Du, Y., Xu, J., Wang, Y., & Lin, T. (2017). Thermoelectric properties of graphite-PEDOT: PSS coated flexible polyester fabrics. Journal of Materials Science: Materials in Electronics, *28*(8), 5796–5801. https://doi.org/10.1007/s10854-016-6250-2
7. Ferhat, S., Domain, C., Vidal, J., Noël, D., & Ratier, B. (2019). AC SC. *Organic Electronics*, *2*. https://doi.org/10.1016/j.orgel.2019.02.031
8. Gao, Y. N., Wang, Y., Yue, T. N., Weng, Y. X., & Wang, M. (2021). Multifunctional cotton non-woven fabrics coated with silver nanoparticles and polymers for antibacterial, superhydrophobic and high performance microwave shielding. Journal of Colloid and Interface Science, *582*, 112–123. https://doi.org/10.1016/j.jcis.2020.08.037
9. Jin, Q., Jiang, S., Zhao, Y., Wang, D., Qiu, J., Tang, D., Tan, J., Sun, D., Hou, P., Chen, X., Tai, K., & Gao, N. (n.d.). a carbon nanotube scaffold. Nature Materials. https://doi.org/10.1038/s41563-018-0217-z
10. Kim, M., Park, D., & Kim, J. (2022). A thermoelectric generator comprising selenium-doped bismuth telluride on flexible carbon cloth with n-type thermoelectric properties. Ceramics International, *48*(8), 10852–10861. https://doi.org/10.1016/j.ceramint.2021.12.302
11. Li, H., Zong, Y., Li, X., Ding, Q., Jiang, Y., & Han, W. (2021). Biodegradable CuI/BCNF composite thermoelectric film for wearable energy harvesting. Cellulose, *28*(17), 10707–10714. https://doi.org/10.1007/s10570-021-04244-4
12. Li, M., Chen, J., Zhong, W., Luo, M., Wang, W., Qing, X., Lu, Y., Liu, Q., Liu, K., Wang, Y., & Wang, D. (2020). Large-Area, Wearable, Self-Powered Pressure-Temperature Sensor Based on 3D Thermoelectric Spacer Fabric. ACS Sensors, *5*(8), 2545–2554. https://doi.org/10.1021/acssensors.0c00870
13. Liu, C., Zhao, K., Fan, Y., Gao, Y., Zhou, Z., Li, M., Gao, Y., Han, Z., Xu, M., & Pan, X. (2021). A flexible thermoelectric film based on Bi 2 Te 3 for wearable applications. Functional Materials Letters,

2251005, 1–6. https://doi.org/10.1142/s1793604722510055

14. Liu, G., & Qiao, G. (2015). *Nanowires as Building Blocks to Fabricate Flexible Thermoelectric Fabric: The Case of Copper Telluride Nanowires*. https://doi.org/10.1021/acsami.5b07144
15. Liu, Y., Chen, J., Deng, H., Hu, G., Zhu, D., & Dai, N. (2016). Anomalous thermoelectricity in strained Bi 2 Te 3 films. Nature Publishing Group, *August*, 2–8. https://doi.org/10.1038/srep32661
16. Lund, A., Tian, Y., Darabi, S., & Müller, C. (2020). A polymer-based textile thermoelectric generator for wearable energy harvesting. Journal of Power Sources, *480*(May), 228836. https://doi.org/10.1016/j.jpowsour.2020.228836
17. Ma, J., Zhao, Q., Zhou, Y., He, P., Pu, H., Song, B., Pan, S., Wang, Y., & Wang, C. (2021). Hydrophobic wrapped carbon nanotubes coated cotton fabric for electrical heating and electromagnetic interference shielding. Polymer Testing, *100*, 107240. https://doi.org/10.1016/j.polymertesting.2021.107240
18. Maria, A., Maji, T., Drew, C., Kumar, J., & Christodouleas, D. C. (2021). High-performance thermoelectric fabric based on PEDOT: Tosylate / CuI. Applied Materials Today, *25*, 101180. https://doi.org/10.1016/j.apmt.2021.101180
19. Nuthongkum, P., Sakdanuphab, R., Horprathum, M., & Sakulkalavek, A. (2017). [Bi]:[Te] Control, Structural and Thermoelectric Properties of Flexible BixTey Thin Films Prepared by RF Magnetron Sputtering at Different Sputtering Pressures. Journal of Electronic Materials, *46*(11), 6444–6450. https://doi.org/10.1007/s11664-017-5671-x
20. Paleo, A. J., Vieira, E. M. F., Wan, K., Bondarchuk, O., Cerqueira, M. F., Bilotti, E., Melle-Franco, M., & Rocha, A. M. (2020). Vapor grown carbon nanofiber based cotton fabrics with negative thermoelectric power. Cellulose, *27*(15), 9091–9104. https://doi.org/10.1007/s10570-020-03391-4
21. Park, K. T., Lee, T., Ko, Y., Cho, Y. S., Park, C. R., & Kim, H. (2021). *High-Performance Thermoelectric Fabric Based on a Stitched Carbon Nanotube Fiber*. https://doi.org/10.1021/acsami.0c20252
22. Poudel, B., Hao, Q., Ma, Y., Lan, Y., Minnich, A., Yu, B., Yan, X., Wang, D., Muto, A., Vashaee, D., Chen, X., Liu, J., Dresselhaus, M. S., Chen, G., & Ren, Z. (2008). High-thermoelectric performance of nanostructured bismuth antimony telluride bulk alloys. Science, *320*(5876), 634–638. https://doi.org/10.1126/science.1156446
23. Tan, Y. J., Li, J., Gao, Y., Li, J., Guo, S., & Wang, M. (2018). A facile approach to fabricating silver-coated cotton fiber non-woven fabrics for ultrahigh electromagnetic interference shielding. Applied Surface Science, *458*(July), 236–244. https://doi.org/10.1016/j.apsusc.2018.07.107
24. Varghese, T., Dun, C., Kempf, N., Saeidi-javash, M., Karthik, C., Richardson, J., Hollar, C., & Estrada, D. (2019). Flexible Thermoelectric Devices of Ultrahigh Power Factor by Scalable Printing and Interface Engineering. *1905796*, 1–8. https://doi.org/10.1002/adfm.201905796
25. Wei, S., Liu, L., Huang, X., Zhang, Y., Liu, F., Deng, L., Bilotti, E., & Chen, G. (2022). *Flexible and Foldable Films of SWCNT Thermoelectric Composites and an S – Shape Thermoelectric Generator with a Vertical Temperature Gradient*. https://doi.org/10.1021/acsami.1c21363

26. Wu, Q., & Hu, J. (2016). Waterborne polyurethane based thermoelectric composites and their application potential in wearable thermoelectric textiles. Composites Part B: Engineering, *107*, 59–66. https://doi.org/10.1016/j.compositesb.2016.09.068
27. Wu, X., & Wen, B. (2021). Vermicular Ni@RL-CS: Preparation, characterization and its applications in electromagnetic shielding. Ceramics International, *47*(20), 28698–28713. https://doi.org/10.1016/j.ceramint.2021.07.029
28. Zhang, X., Li, T., Ren, H., Peng, H., Shiu, B., Wang, Y., Lou, C., & Lin, J. (2020). *Dual-Shell Photothermoelectric Textile Based on a PPy Photothermal Layer for Solar Thermal Energy Harvesting*. https://doi.org/10.1021/acsami.0c16401
29. Zhao, Y., Li, Y., Qiao, J., Jiang, S., & Mao, P. (2020). Decoupling phonon and carrier scattering at carbon nanotube / Bi 2 Te 3 interfaces for improved thermoelectric performance. Carbon, *170*, 191–198. https://doi.org/10.1016/j.carbon.2020.08.024

Figures

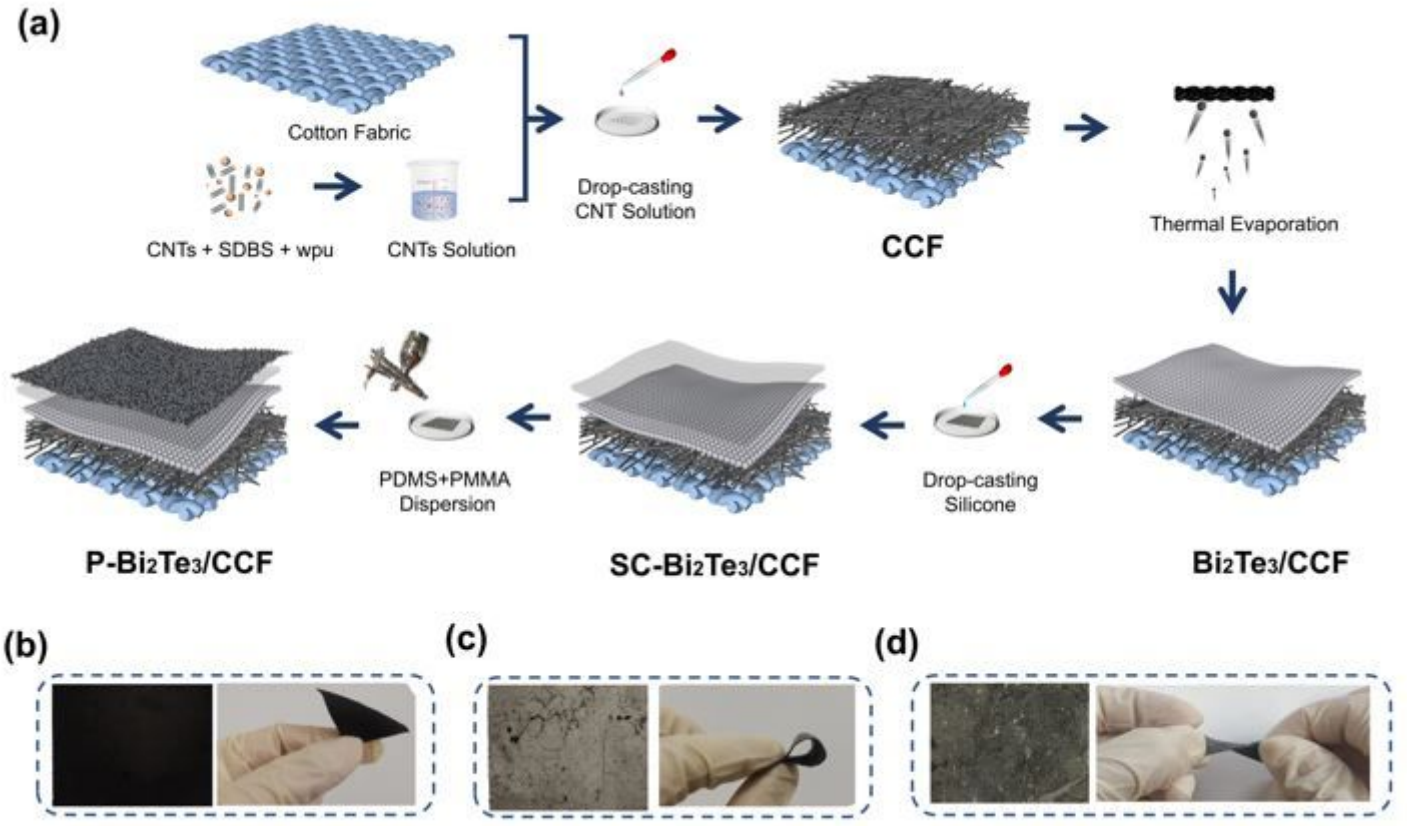

Figure 1

(a) Schematic illustration of the fabrication of the P-Bi2Te3/CCF. Digital photograph of (b) CCF conductive fabric, (c) Bi2Te3/CCF thermoelectric fabric and (d) P- Bi2Te3/CCF Superhydrophobic thermoelectric fabric.

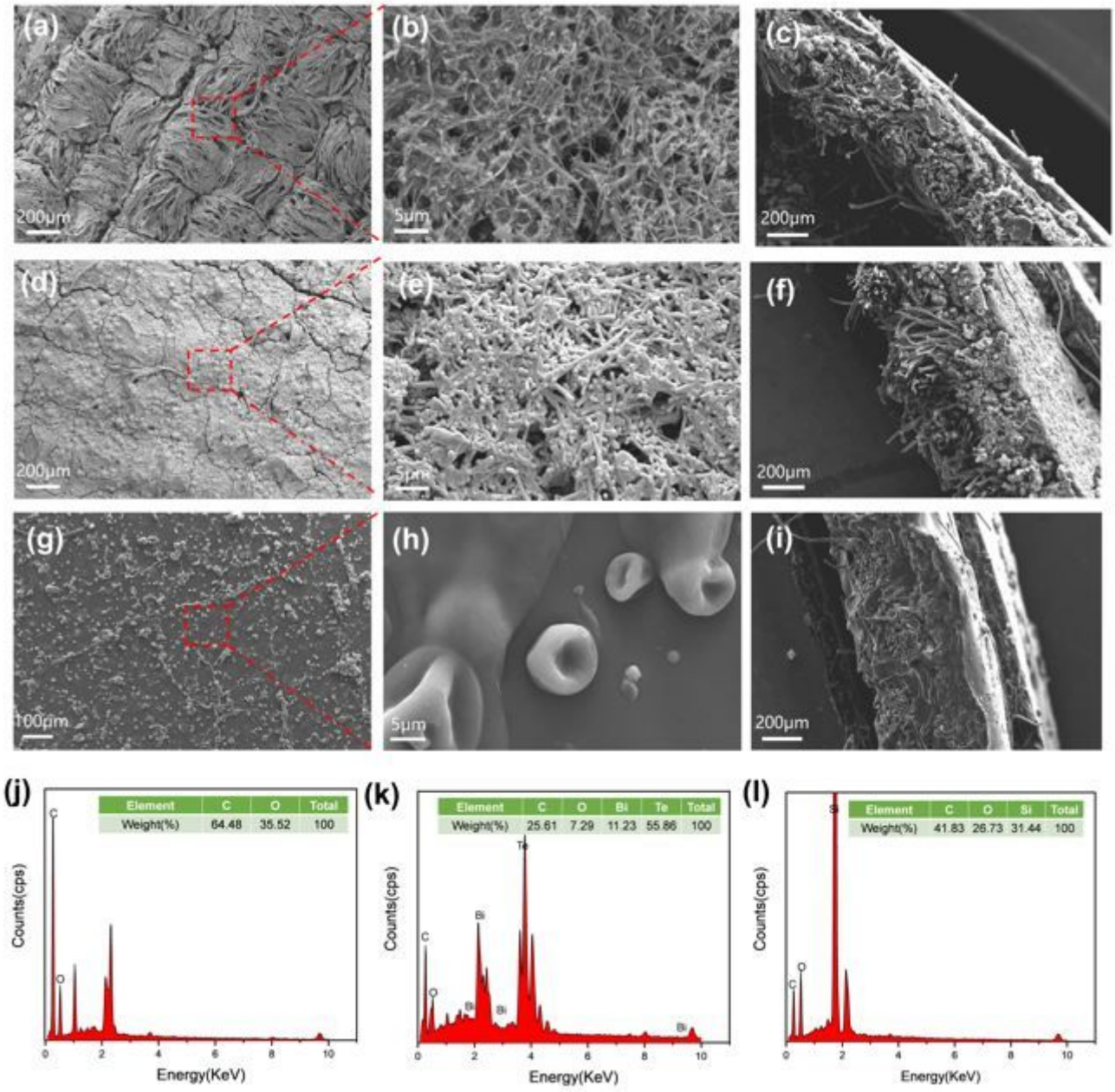

Figure 2

Surface SEM images of (a, b) the CCF, (d, e) the Bi2Te3/CCF and (g, h) the P-Bi2Te3/CCF. Cross-section SEM images of (c) the CCF, (f) the Bi2Te3/CCF and (i) the P-Bi2Te3/CCF. X-ray energy dispersive spectrum and element weight percentage of (j) the CCF, (k) the Bi2Te3/CCF and (l) the P-Bi2Te3/CCF.

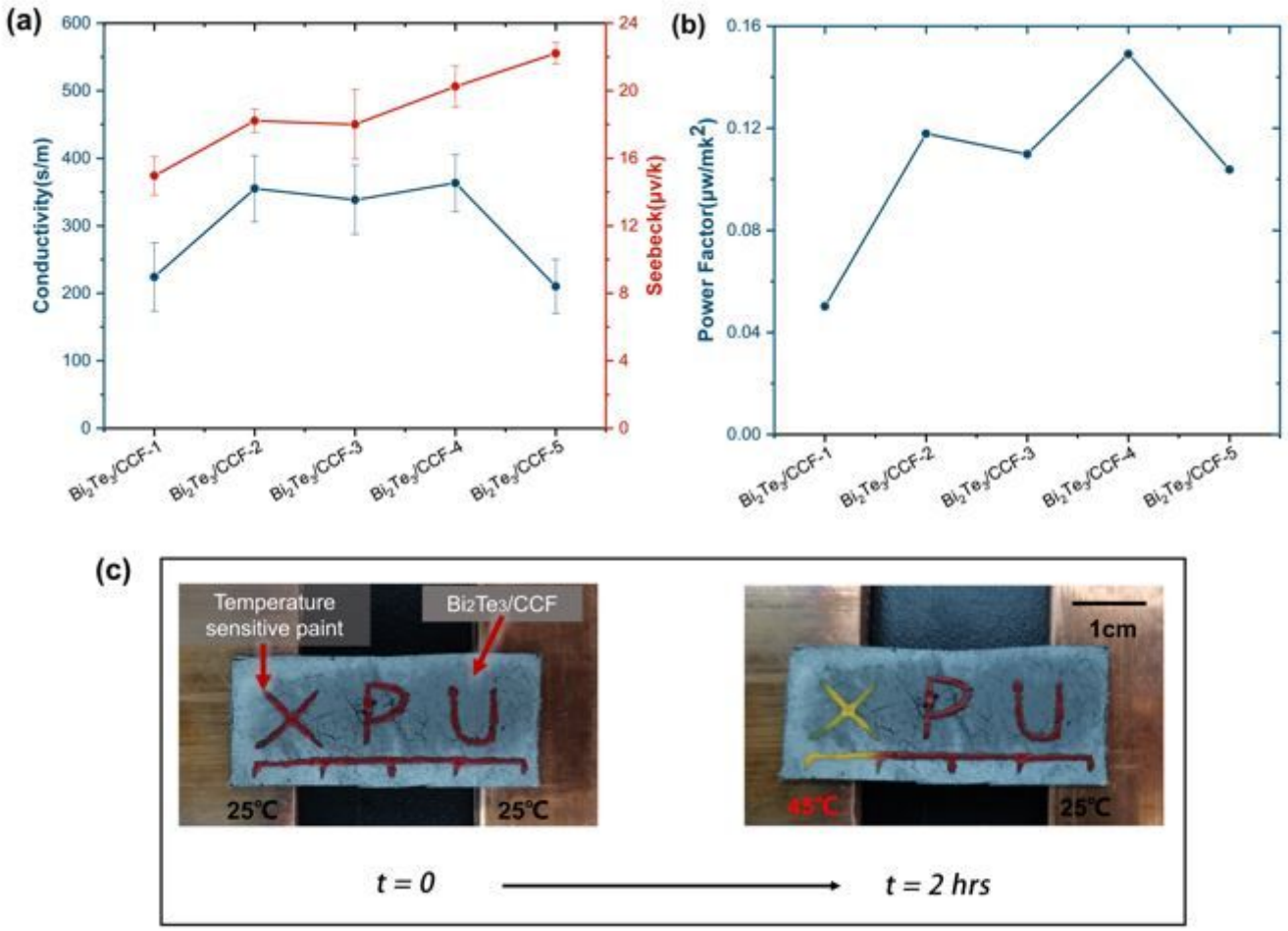

Figure 3

(a) The Seebeck coefficient and conductivity of Bi2Te3/CCF, where TC is measured at 25 °C. (b) Thermoelectric power factor of Bi2Te3/CCF, where TC is measure at 25 °C. (c) Thermochromic paint visualizes lateral (in-plane) heat transfer across a Bi2Te3/CCF.

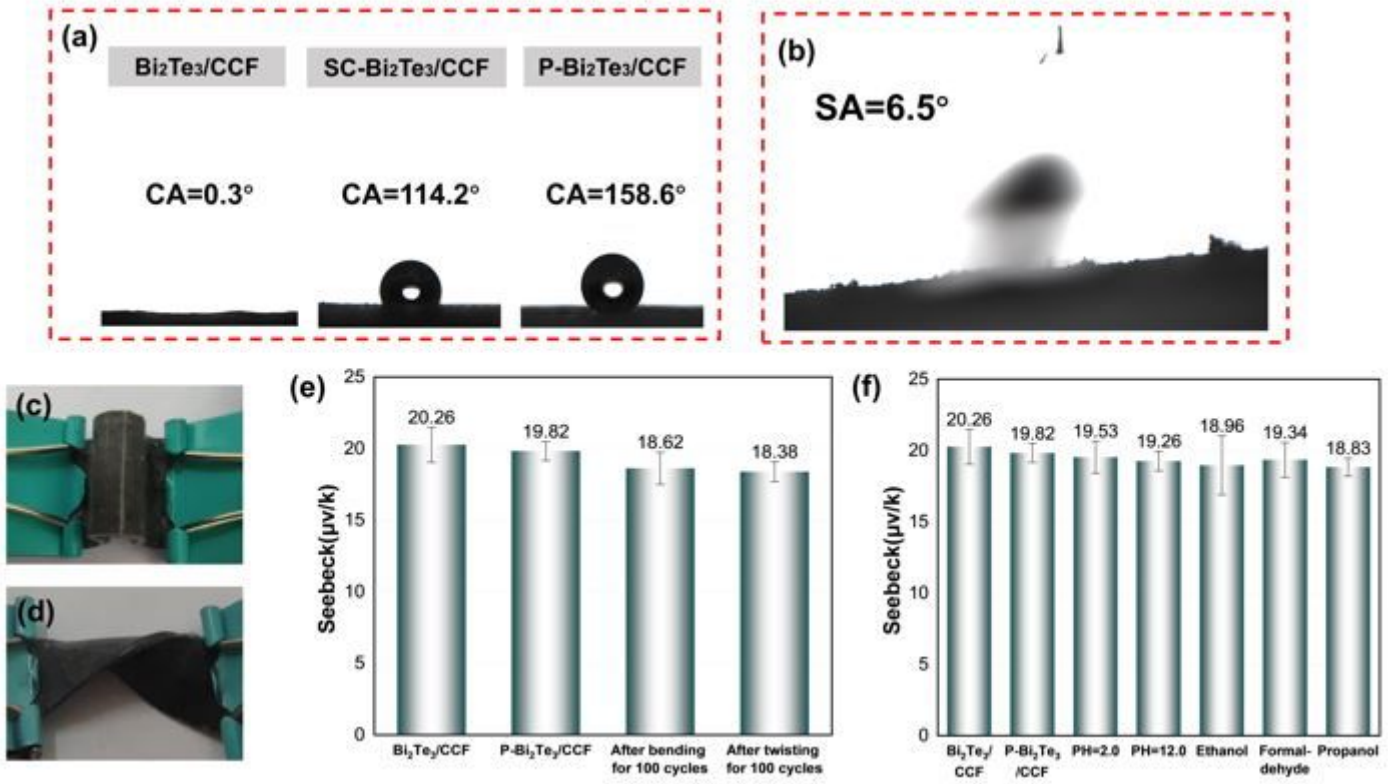

Figure 4

(a) The optical images of CA for the Bi2Te3/CCF, the SC-Bi2Te3/CCF and the P-Bi2Te3/CCF. (b) The optical images of SA for P-Bi2Te3/CCF. (c) The bending state of one P-Bi2Te3/CCF specimen with a bending radius of 2.0 mm. (d) The twisting state of one P-Bi2Te3/CCF specimen at a twisting angle. (e) conductivity changes of P-Bi2Te3/CCF before and after repeatedly bending-release and twisting-release for 100 cycles, respectively. (f) conductivity changes of P-Bi2Te3/CCF before and after immersing the specimens into acidic solution (PH = 2.0), alkali solution (PH = 12.0) and various organic solvents for 10 h, respectively.

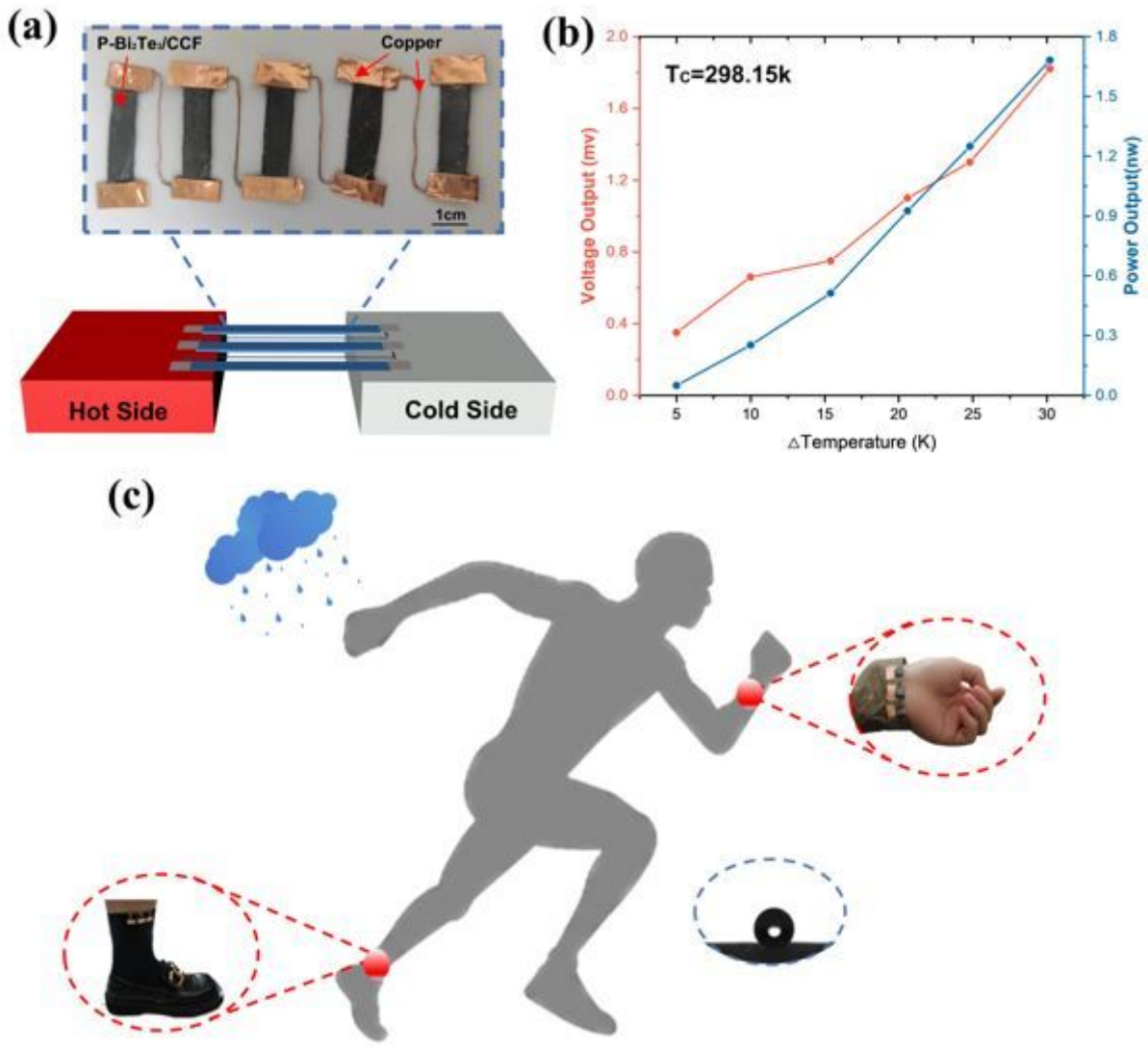

Figure 5

(a) The thermoelectric measurement setup and architecture of the prepared TEG. (b) Thermoelectric output performance of the TEG. (c) Demonstration of wearing the TEG, and the water contact angle of superhydrophobic encapsulation.

Supplementary Files

This is a list of supplementary files associated with this preprint. Click to download.

- 1658824087328798.mp4
- supportinformation.docx